PAPER Nr.: 62

ANALYSIS OF A 1/6 SCALE EUROFAR SEMI-SPAN WIND TUNNEL MODEL, FOR AEROELASTIC STABILITY AND LOADS

BY

P T W JUGGINS

WESTLAND HELICOPTERS LIMITED

YEOVIL, ENGLAND

TWENTIETH EUROPEAN ROTORCRAFT FORUM
OCTOBER 4 - 7, 1994 AMSTERDAM

Printed by the Technical Highschool Haarlem

ANALYSIS OF A 1/6 SCALE EUROFAR SEMI-SPAN WIND TUNNEL MODEL, FOR AEROELASTIC STABILITY AND LOADS

P T W JUGGINS
WESTLAND HELICOPTERS LIMITED

ABSTRACT

The design, testing and analysis of a 1/6 scale, half tip speed semi-span model of a tilt-rotor, comprising of a prop-rotor, nacelle and wing, were performed as part of the EUROFAR Phase One tilt-rotor study (a EUREKA Project), for investigation of aeroelastic (whirl-flutter) stability, as well as loads measurements. The design and test of the model has previously been reported, with comparisons with initial stability predictions. In this current paper, the analytical bases of the model activity are described, in respect of both the analysis of the test data and the application of prediction methods and their correlation with test.

The component structures of the stability and loads prediction methods are described. Different standards of theoretical model for stability are examined, and conclusions are draw as to the level of modelling required, and the sensitivity of results to selected parameters. Correlations of cruise stability with predictions based on the 'best' modelling assumptions and alternative assumptions are presented. Comparisons of measured blade loads in the conversion regime with predictions are also assessed. Overall agreement levels for both stability and loads are encouraging.

1 INTRODUCTION

The design and test of the model (Figure 1) were reported in Reference 1, together with initial stability predictions. The measurements made form a basis for validation of prediction methods for use in tilt-rotor design, for the EUROFAR aircraft in particular. The model was the third in a series of strategically defined wind tunnel models for EUROFAR, the others being a drag model and an aerodynamic performance model (Reference 2), and is therefore designated Model 3. Stability measurement during the tests was made by application of the Moving Block method to decaying signals following excitation of the rotor cyclic or collective pitch at mode frequencies of interest. A requirement was identified to re-analyse the decays at Westland Helicopters Limited (WHL) to reduce scatter in torsion and chord mode damping estimates, applying the Moving Block to blade strain gauge signals, rather than those from wing accelerometers. Additional data not analysed previously at the test were to be included.

In the tests, the whirl-flutter stability boundary in cruise was successfully approached and defined for five different rotor configurations. Data were also obtained from conversion regime cases, with the rotor tilted with respect to the air flow, to extract blade loads for assessment and comparison with prediction. Stability

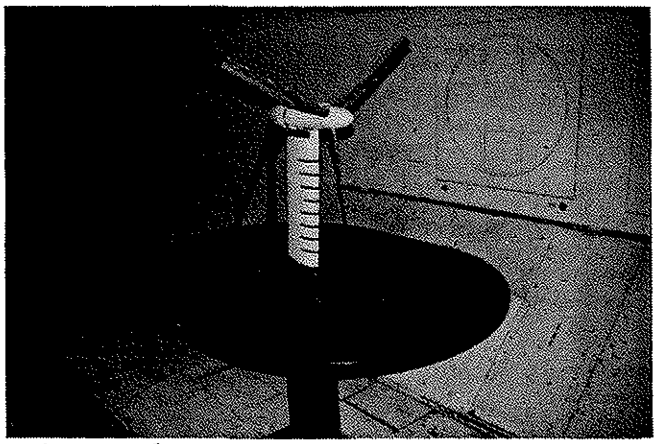
Figure 1

predictions have been made subsequently, using the WHL Coupled Stability Analysis (CSA), also described in Reference 3. The blade loads predictions have used an adaptation of a well-proven analysis for helicopter rotors, the Westland/DRA Coupled Modes Performance Program R150 (References 4 and 5). This paper presents the improved test data analysis, reviews the prediction methods, and considers the agreement achieved between prediction and test, with reference to sensitivity to modelling assumptions.

2 POST-TEST APPLICATION OF THE MOVING BLOCK ANALYSIS

At the test site, wing-tip accelerometers were used to provide the signals for the damping evaluation of the wing modes, while measurements for the blade lead-lag mode were obtained using blade strain gauges. Wing beam and chord modes were evaluated using the tip accelerometers oriented in those respective directions, while the blade torsion mode was evaluated using the chordwise accelerometer. As wind tunnel speed was increased, damping levels in the chord and torsion modes increased, and modal excitation levels were increasingly limited by allowable blade strains, rather than by wing motion. Results from the Moving Block for these modes (for torsion in particular) showed significant scatter in damping. Previous experience has shown that the accuracy and repeatability of the Moving Block method is degraded as damping levels increase and as the response is reduced relative to other signal content (Reference 6, for example). In order to utilise increased response levels, it was determined that damping levels of the wing chord and torsion modes should be derived from the blade strain gauge data in post-test analysis, with an appropriate transformation into the non-rotating frame of reference.

In order to perform the further analysis of the test data at WHL, a dedicated program (MBLOCK) was configured to select and read the records (from 500 megabytes of stored data on hard disk) and apply the Moving Block method. This program also provided the basis for code to evaluate mode shapes from the data and to extract loads waveforms. The MBLOCK analysis, followed the approach in Reference 7. The full set of wing chord and torsion mode data was analysed using MBLOCK. Results were available for five rotor configurations; combinations of rotor speed, thrust and delta-3 coupling geometry (Table 1).

Table 1 Test Configurations

Rotor Speed (rpm)	Nominal Thrust (N)	Delta-3 (deg)
900	0.0	0.0
900	67.0	0.0
1124	0.0	0.0
900	0.0	20.0
900	67.0	20.0

Thrust values for the conditions tested were "nominal", since unresolved inaccuracy in measurement of thrust led to the use of measured rotor torque to set the conditions (Reference 1). An assumption of 80% cruise efficiency was used to define a target torque corresponding to the nominal 67 N thrust (a scaled value for cruise), while zero torque was used for the nominal zero thrust points (or, at zero wind, minimum torque).

Typical derived chord and torsion mode damping results for 900 rpm, 'zero thrust' and zero delta-3 are shown in Figures 2 and 3. The MBLOCK results are from strain gauges on the metallic flexure at the inboard end of the blade (Reference 1). Edgewise gauge records were used at lower wind speeds, and flatwise gauge records at higher speeds, reflecting the effect of increasing pitch on resultant lead-lag response. At zero wind, the wing-tip accelerometer records were used, since the lead-lag response was much smaller. Also plotted on the Figures are the original results from on-site analysis, from the wing-tip accelerometers, and some results for data which were not analysed at the test site.

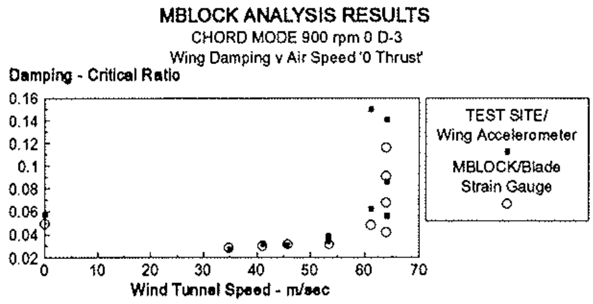

Figure 2

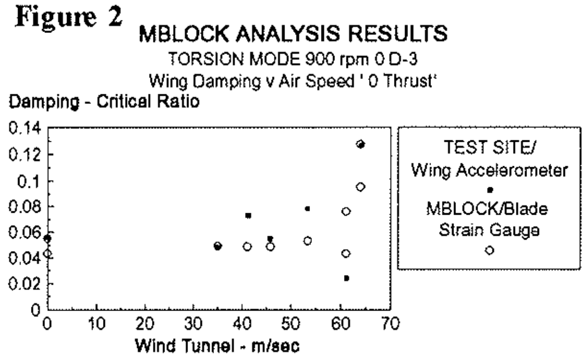

Figure 3

In general, the most benefit from the application of MBLOCK to the gauge data was seen in reduced scatter in torsion mode results. This reflects the limited response of the chordwise wing-tip accelerometer to wing torsional motion, particularly relative to blade strains at high speed. For most cases chord mode results from the on-site analysis were confirmed by the application of MBLOCK. In Figure 2, the inherent limitations in obtaining repeatable damping results from the Moving Block method at higher levels of damping (4% or more) are demonstrated.

3 DESCRIPTION OF THEORETICAL ANALYSES

Prediction methods used included WHL computer programs J134 (for blade modes), J169/CSA (for stability) and R150 (for blade loads). Data for correlation with these analyses were obtained respectively from blade rap tests, from measured frequencies and damping in the wind tunnel and from measured blade loads in the conversion regime. Natural frequencies and mode shapes of the non-rotating structure were predicted using NASTRAN finite element modelling. These were also measured in a simple shake test.

3.1 Blade Modes Prediction (J134)

The WHL blade modes program J134 has been extensively applied to helicopter rotor systems over at least 14 years, during which it has continued to be refined. Example applications are given in References 3, 4 and 5. The analysis is for computation of the natural frequencies and mode shapes of a shaft-fixed single blade rotating at constant angular velocity. The blade may be twisted, and the locus of cross section shear centres may be modelled by up to 24 straight segments. Properties defined at each cross section include full mass-centre and tension-centre offset descriptions, and deformation is described by 3 translations and 3 slopes, typically at 900 integration points. The blade model may have a variety of root hinge conditions and secondary load paths, including transmission and control system impedance models. The modes are calculated for the blade about a steady deflected state under given steady external load distributions, which may be defined by an aerodynamic model within the program. Both steady-state and perturbatory (modes) solutions of the equations of motion are by the Transfer Matrix method. Cross-sectional mass and stiffness properties for the Model 3 blades were confirmed by measurements during the blade design and manufacture. The properties were maintained at 1/6 dynamically scaled values based on a full-size EUROFAR specification, with the exception of some stiffnesses increased for practical reasons in the tip region.

During the Model 3 test activity, rap tests of blades were performed, both in a hub-clamped condition and in-situ. Agreement of the J134 predictions with the test results was very good, with an average absolute difference between hub-clamped frequencies and predictions of +1.1% (2.1% based on magnitude) for the first 6 modes, and between in-situ frequencies and predictions of -0.7% (3.5% based on magnitude) for 8 modes.

3.2 Stability Prediction (CSA)

The WHL Coupled Stability Analysis (CSA) was initially developed to predict the stability margins for tilt-rotor whirl-flutter in cruise or conversion regimes, but has subsequently been further developed and applied (Reference 3). The components of the model include:

Fuselage with fully-coupled motions.
Gimbal joint, with stiffness and damping.
Blades with fully-coupled motions.
Transmission (not used for Model 3).
Conversion case simulation, with cyclic pitch.

The fuselage dynamic behaviour is described by a set of fuselage modes(usually obtained from a finite element model). The modes are input as a set of modal frequencies, inertias and damping values, together with mode shapes defined at the rotor hub point. The degrees of freedom for the fuselage used within CSA are then the mode generalised coordinates (ie modal responses). The fuselage model usually includes a rotor mass representation, which is subsequently subtracted by CSA prior to its addition from the blade modes. The position and orientation of the gimbal/hub can then be expressed, given all 6 components of motion in the modes at the hub point, by a modal summation. The gimbal joint is modelled by 2 orthogonal rotational freedoms with associated inertia, stiffness and damping, the 2 freedoms being identical. The rotor rotational velocity is then taken to be in the plane, the normal of which is the output drive shaft from the gimbal to the rotor (ie the gimbal is a homokinetic drive). The blade dynamic behaviour is described by a set of fully coupled (flap-lag-torsion) blade modes from program J134, calculated for the case where the blades are considered built-in at the root. The effects of collective and cyclic couplings are accounted for by the rest of the system to which the blades are attached in CSA. As with the fuselage, equations in mode generalised coordinates are configured in CSA, but for the blade these include mode inertial coupling terms due to velocity. Aerodynamic loads are found using quasi-static theory. The program has recently been extended to include the option of unsteady aerodynamics as described in Reference 3, which also includes correlation of CSA against tests and other analyses, for blade stability.

For Model 3, four nacelle/wing modes (- fundamental beam, chord and torsion, plus the zero-frequency transmission mode) and two blade modes (- fundamental flap and lag) were used in CSA. Studies showed that including further modes had a negligible effect on stability predictions.

3.3 Blade Loads Prediction (R150)

R150 is a well-established program for the prediction of helicopter rotor loads, developed over several years by WHL and DRA (UK Defence Research Agency). Correlation exercises using R150 include those documented in References 4 and 5. Like CSA, the analysis uses blade modal degrees of freedom, with blade modes supplied by program J134.

For the Model 3 activity, application of R150 to the tilt-rotor was sought with minimum modifications to the analysis, since the bulk of resources used in the project were to be aimed at the primary objective of validation of aeroelastic stability predictions. Loads measurement and correlation with theory were secondary objectives, and there was also a requirement for loads prediction in the design process for the model blades and hub. The unique features of the tilt-rotor were identified as the effect of the wing on rotor aerodynamics and the hub gimbal. A version of R150 was therefore modified to include a wing circulation model. The gimbal was represented by using 2 different sets of modes from J134 (each of 8 modes), with built-in (symmetric) and teetered (asymmetric) root conditions respectively. The teetered root condition included the gimbal stiffness (per blade) as a spring. Loads for each mode set were calculated in R150. The resultant blade loadings were then synthesised by combining harmonics from the symmetric and asymmetric cases appropriately, as follows:

Harmonic	0(steady)	1	2	3	4	5	6	7	8	9
Synthesis (3 blades)	S	A	A	S	A	A	S	A	A	S
Synthesis (4 blades)	S	A	S*	A	S	A	S*	A	S	A

S - symmetric modes A - asymmetric modes (* - reactionless)

For Model 3, the 3-bladed synthesis was used. It was recognised that the teetered root condition did not accurately represent the homokineticity of the gimbal, and hence that some discrepancy in lead-lag loads might be expected, due to Coriolis effects. A further approximation was necessary to model the NACA 64 Series aerofoils used on the Model 3 blade, which are not on the WHL aerofoil library for unsteady properties required in R150's indicial aerodynamics. As a first approximation, NACA 0012 section characteristics were used. Of particular interest in this study was the level of correlation of R150 predictions with tilt-rotor blade loads which could be obtained taking this minimum-modification approach.

3.4 Structural Dynamics Models

For calculations of stability in the EUROFAR Preliminary Project Phase for the full-scale baseline aircraft, considerable care had been taken to include sufficient detail in the structural dynamics model, particularly with respect to wing root conditions. Modes for input to CSA were obtained from a full-span NASTRAN finite element model, illustrated in Figure 4.

For Model 3 the basis of the structural dynamics modelling was again a NASTRAN representation. Model 3 was a half-span wing and nacelle mounted on a test stand with a substantial pipe-like structure (Reference 1). The wing consisted of a composite spar within a foam-filled wing profile slit into short sections to minimise its effect on stiffness. The wing also contained a drive shaft. The nacelle consisted of a non-tilting cradle-like structure supporting a tilting gearbox and rotor shaft, with a hydraulic tilt actuator. A facility to adjust the stiffness of the tilt-actuator mounting was included by use of interchangeable torsion bars. For the wind tunnel test only the stiffest bar was used. A relatively simple NASTRAN representation of Model 3 was configured, typically using 56 grid points connected by beam and rigid elements, and including concentrated masses and point springs. A transmission system model was included, modelling the effects of drive-shaft bending and the coupling of wing bending with shaft rotation via the 2:1 right-angle gearbox.

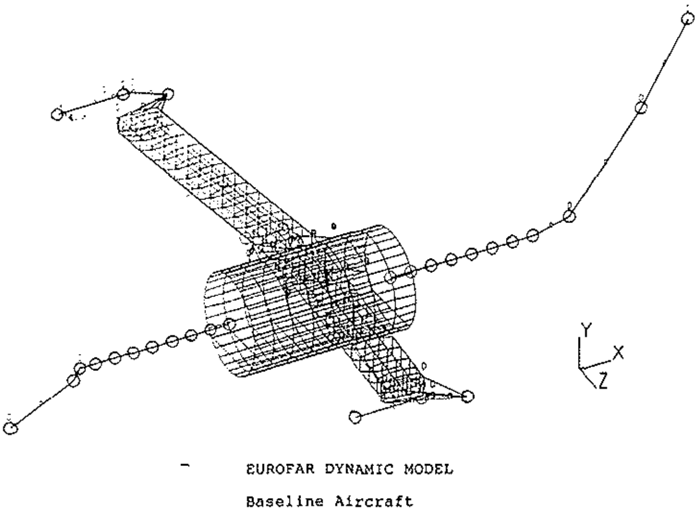

Figure 4

The model is illustrated in Figure 5, where the fundamental wing beam mode shape is shown overlaid on the undeflected condition. The blade representations are rigid massless elements for visualisation purposes only. While the test stand and wing representations were essentially by beam elements, the nacelle was originally assumed to be rigid apart from the tilting mechanism spring, which for the configuration tested was relatively rigid. The nacelle mass distribution was represented by forward and aft or single concentrated masses and inertias, depending on the standard of model, based initially on weight calculations and subsequently also on a measurement of total nacelle weight, pitching inertia and cg position. The rotor was represented by a further concentrated mass.

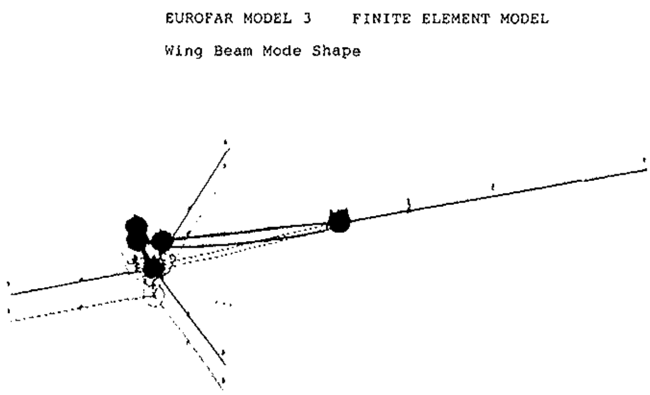

Figure 5

The structural dynamics model was developed and modified such that 6 main versions were used in the studies (see section 4.1, below). These were designated as follows:

Designation	Description
N*	Basic pre-test standard (stiff torsion bar).
N	Post-commissioning standard, with frequency tuning.
S	Shake test modes.
X	With simple nacelle (tilting) flexibility and measured nacelle mass/inertia properties.
Y	With nacelle tilting mechanism model.
UN	Reduced-coupling mode set based on X, for parameter identification studies.

A simple shake test of the model was performed prior to the commissioning in the wind tunnel, with a dummy rotor mass installed. Frequencies were also measured at zero wind speed in a flutter check in the wind tunnel, in which the rotating dummy rotor mass was used to excite the wing modes in turn via out-of-balance forces. Frequencies from the flutter check and shake test are given in Table 2, together with equivalent results from the theoretical structural models.

Table 2 Wing Natural Frequencies (With Rotor Mass Only)

	FREQUENCIES (HZ)				DAMPING (%CRIT)		
	BEAM	CHORD	TORSION		BEAM	CHORD	TORSION
Flutter Test:	4.44	5.38	6.91		0.5	2.3	1.7
Shake Test:	4.6	5.9	7.6				
Models:							
N*	5.49	6.55	8.78	* pre-test			
N	4.58	5.45	7.33				
X	4.56	5.40	6.76				
Y	4.57	5.35	6.33				
UN	4.54	5.38	6.11				

Overall, the X-standard structural model gives the best frequency agreement with measurements from the flutter check. There was some doubt over the validity of shake test results, since significant stiction was discovered in the tilting mechanism bearings subsequent to the shake test, with a consequent effect on torsion frequencies. Evidence had shown that the wing torsion frequency fell by around 0.5 Hz after commissioning trials and the shake test, following work to reduce the excessive friction prior to the flutter check and the full wind tunnel test.

4 SENSITIVITY STUDIES OF THEORETICAL MODEL

Evaluation has been performed of the parameters within the theoretical stability model which influence the level of agreement with test. This work falls into 2 categories. Firstly, the influence of the non-rotating structure has been examined, with the development of a set of alternative models. Additionally, other key parameters have been assessed, namely those of aerodynamic blade tip loss, the effect of wing aerodynamics, the assumption of a single blade mode set used over a tunnel speed range against multiple sets and the influence of assumed gimbal stiffness.

4.1 Structural Parameters

While the importance of an adequate stability analysis for the total coupled rotor-wing system is clear, the use of a valid model of the dynamics of the non-rotating structure within that analysis is a prerequisite for successful predictions. In Reference 8, it was concluded that errors in a NASTRAN model of the XV-15 aircraft and uncertainties in the estimation of structural damping were at least as important as differences between stability prediction methods (in this case the ASAP and CAMRAD codes).

4.1.1 Standards of Structural Model

Following the initial commissioning of Model 3 in the wind tunnel, it was apparent that the frequencies given by the non-rotating (NASTRAN) structural model were too high. Simple tuning of the model by a point spring at the wing root to allow for unknown rig flexibility gave good agreement with the commissioning frequencies (see Table 2), with this structural model designated the 'N' standard. Subsequently, after the wind tunnel test itself, a further revision of the model was necessary, to allow for the apparent (unpredicted) softening in torsion due to removal of stiction in the tilting mechanism. This new 'X' standard model was achieved by simplifying the nacelle mass and inertia modelling to match measured (rather than estimated) properties, and introducing a wing-tip spring to model the unknown nacelle tilting flexibility. This gave a model with good torsion frequency agreement without the rotor (Table 2).

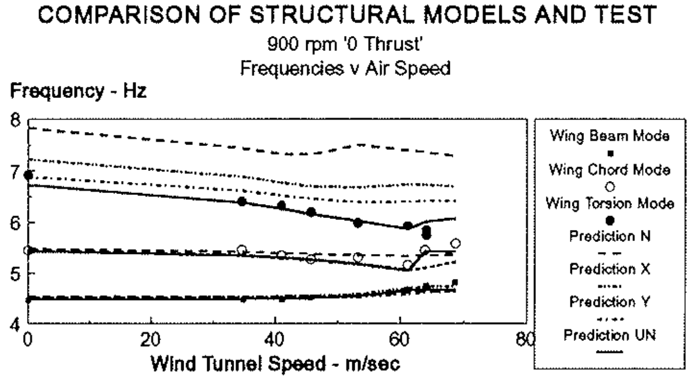

Figure 6

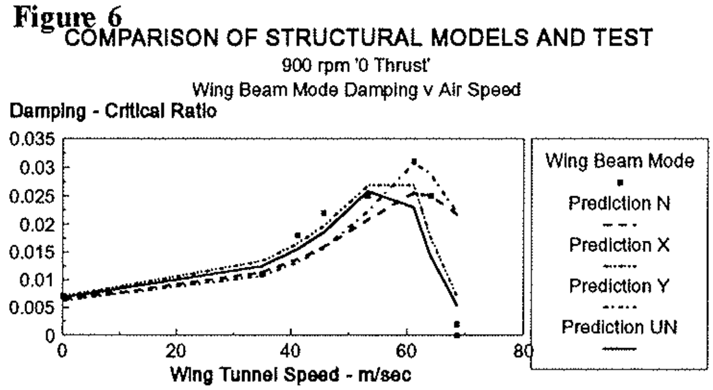

Figure 7

Predicted frequency and damping results from the stability analysis are plotted in Figures 6 and 7 against test, for the 900 rpm, zero delta-3, 'zero thrust' conditions, for models N and X, together with results from further model standards 'Y' and 'UN'. Although the X standard model gave good torsion frequency agreement with the wing flutter check data (from the wing with a dummy rotor mass), addition of the rotor in the analysis gives a stiffening effect due to gimbal opposition motion in the mode, so that the model is too stiff in torsion at zero wind. While beam mode damping results from the X standard are good, the torsion frequency agreement is poor throughout the speed range.

In order to address the discrepancy in torsion frequency, a further NASTRAN model was configured, designated the 'Y' standard. In this, a flexibility was introduced between separately defined tilting and non-tilting nacelle structures, to model the tilting-mechanism load path. The representation used a single spring between rigid elements, and the allocation of inertias between tilting and non-tilting parts of the nacelle was based on estimates. Motion across the tilting mechanism had been detected during the wind tunnel tests, by the tilt-angle potentiometer. Analysis of the data showed that the proportion of the absolute nacelle torsion angle seen across the mechanism varied from 10% to practically zero, dependent on the status of the locking-pin, although corresponding stability results showed no trend due to locking pin status. The Y model was configured to give the maximum 10% proportion in the torsion mode shape. Agreement with the measured torsion frequencies was improved (Figure 6), partly due to improved model tuning, but beam mode damping, although closer to the measured maximum than the N model, was worse than for the X model.

Both the Y model results and the effect of locking pin status on the test results indicate that the unknown flexibility in the nacelle, which was introduced at least in part when the tilting and tilt mechanism bearings were freed, was not simply a flexibility in the tilting freedom between the fixed and tilting parts of the nacelle. Additionally, modifying the structural models had shown that small changes in couplings in the mode shapes, and in the torsion frequency, could have a significant effect on the stability results (see below). Since it was recognised that the accuracy of the existing structural models was limited, a further basis for validating the stability prediction method by a parameter identification approach was defined. A simplified structural model based on the X standard was optimised with respect to agreement of predicted frequencies and damping with test, taking selected motion couplings in the mode shapes and the torsion frequency as the degrees of freedom. As the optimisation used the 900 rpm 0 delta-3 "0 thrust" cases only, two criteria for validation would be available: firstly, the ability to match the data in the optimisation, and secondly, the subsequent agreement of the model for rotor cases not in the optimisation (ie with 20° delta-3, or non-zero thrust).

The optimised model from the parameter identification approach was designated the 'UN' standard. Mode shapes at the rotor hub for the X and UN standards are given in Table 3.

Table 3 X and UN Standards of Structural Models - Wing Mode Shapes at Rotor Hub

	BEAM		CHORD		TORSION	
	X	UN	X	UN	X	UN
Freq.(Hz)	4.56	4.54	5.40	5.38	6.76	6.11
Inertia	0.833	0.830	0.278	0.280	0.0687	0.0700
TX(beam)	1.00	1.00	0.7609	0.6276	1.00	1.00
TY	0.0646	0.0	-0.3644	0.0	0.0960	0.0
TZ(chord)	-0.1785	-0.2299	1.00	1.00	-0.2632	-0.2566
RX	-0.0047	0.0	0.0267	0.0	-0.0070	0.0
RY(torsion)	-0.0686	-0.0700	0.0402	0.0383	0.0677	0.0700
RZ	0.0008	0.0	-0.0004	0.0	-0.0007	0.0

The stability results had been found to be insensitive to the couplings omitted in the simplification for the UN model, while the important beam/torsion and torsion/beam couplings were retained at X-standard values. The process of optimisation of the model was achieved by manual perturbation followed by the application of a genetic method. For the latter, the fit to test data was weighted to favour the frequencies and beam mode damping at the higher wind tunnel speeds. The UN standard results in Figures 6 and 7 show good agreement with both frequencies and beam mode damping. The behaviour of the wing chord mode frequency is particularly well captured by this model.

4.1.2 Individual Effects

In order to illustrate the individual effects of couplings and the torsion frequency, the following matrix of cases was run:

	Parameters			
Case	Torsion Frequency	Torsion in Beam Mode	Chord in Beam Mode	Chord in Torsion Mode
0	datum	datum	datum	datum
1	+5%	datum	datum	datum
2	datum	-10%	datum	datum
3	datum	+10%	datum	datum
4	datum	datum	-10%	datum
5	datum	datum	datum	+10%

The datum model used was the UN standard. For comparison the values of these parameters (at the rotor hub) for the four standards of structural model were:

		Parameters		
Model	Torsion Frequency	Torsion in Beam Mode	Chord in Beam Mode	Chord in Torsion Mode
N	7.32	-0.044	-0.107	-0.196
X	6.76	-0.069	-0.178	-0.263
Y	6.33	-0.053	-0.133	-0.318
UN	6.11	-0.070	-0.230	-0.257

The results of cases 0 to 3 are plotted in Figures 8 and 9, in terms of predicted wing mode frequencies and beam mode damping against airspeed, respectively, with test results. It can be seen that the torsion frequency change (case 1), apart from the direct effect on resultant torsion frequency, affects the shape of the chord frequency plot at high speed, tending to remove the step seen in test, but has little effect on beam mode damping. The torsion coupling changes (cases 2 and 3) also have a (lesser) effect on chord frequency, and have a strong effect on beam damping. It can be seen from Figure 9 that the torsion coupling for the datum case 0 provides a good capture of both the rise and fall of damping, while case 3 predicts the speed for instability better but places the rise and fall less well. Results for cases 4 and 5 showed that the chord couplings in the beam and torsion modes have the effect of "fine-tuning" the predicted chord and torsion frequencies, with little effect on beam frequency or damping. Since the chord and torsion mode damping values are significantly greater than beam at the higher airspeeds, and therefore more difficult to measure accurately, they were omitted from these comparisons.

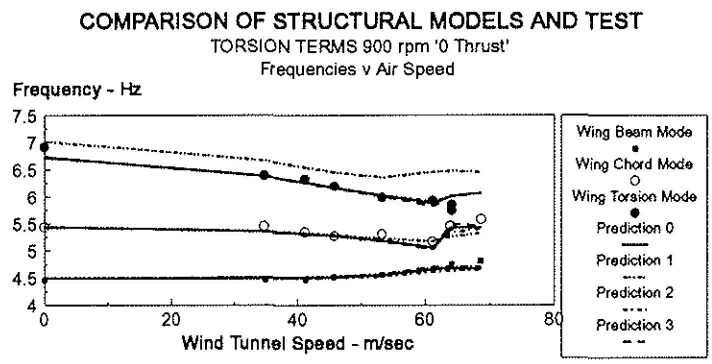

Figure 8

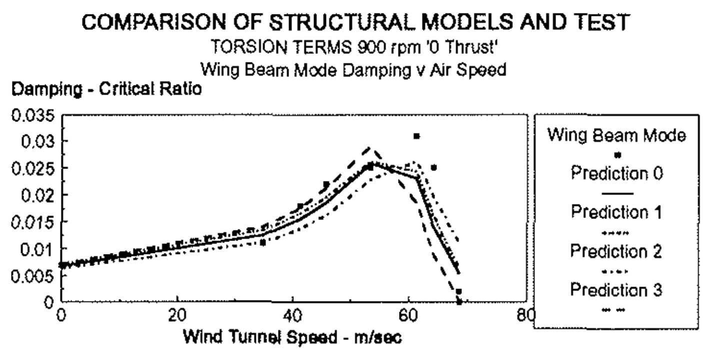

Figure 9

4.2 Blade Tip Relief

In helicopter blade stability prediction analyses it is common practice to use a tip relief value, to define the fraction of rotor radius at which the oscillatory lift is assumed to fall away. In CSA a value of 0.97 is normally used (Reference 3), beyond which the lift is linearly reduced to zero at the tip. The tip relief factor is an allowance for the effect of the shed tip vortex, in the absence of a wake model.

Results in Figures 10 to 12 show the effect of relaxing this assumption, to a factor of unity, on predicted frequencies and damping. In Figure 10, the effect on frequencies is to change the characteristics of the chord and torsion modes at high speeds, around the "step" in chord frequency. Since this area is associated with the crossing of a highly-damped rotor regressing mode (see

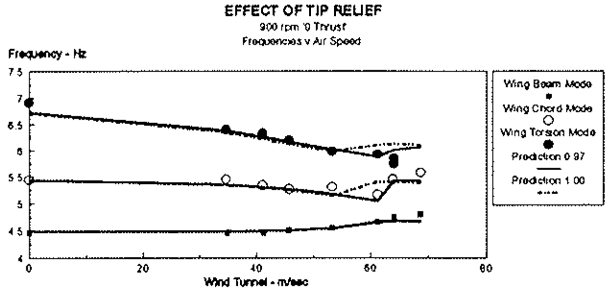

Figure 10

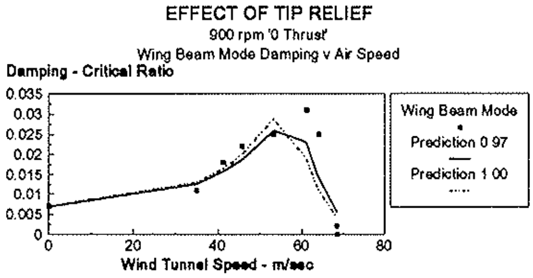

Figure 11

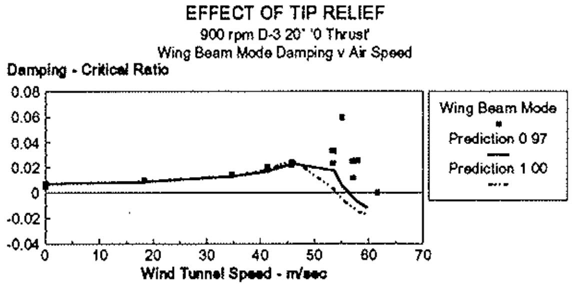

Figure 12

below), sensitivity to the magnitude of the aerodynamic flapping moment is to be expected. The effect on damping for this case (Figure 11) is a small destabilising effect at the highest speed, associated with an earlier damping rise. The effect is more noticeable for the 20° delta-3 case (Figure 12). This is to be expected, since the strength of the aerodynamic stiffness term from delta-3 is increased by removal of tip relief, and the results already show that this term is destabilising. From these results, better agreement with test is obtained with the tip relief factor of 0.97.

4.3 Wing Aerodynamics

Stiffness and damping terms from wing aerodynamics are not included in CSA, on the basis that tilt-rotor design constraints, not least for whirl flutter, drive wing properties well away from classical flutter or divergence boundaries for speeds of interest, such that these terms are not significant.

Noting that the wing stiffnesses of Model 3 are not dynamically scaled from full-size (Reference 1), a flutter check up to maximum tunnel speed (84 m/s) was carried out, using a rotating dummy rotor mass. The damping trends were flat, with some scatter of results, up to the maximum rotor-on speed of the tests of 68.6 m/s. Above this speed there was evidence of a drop in torsion mode damping. The incremental damping above zero-wind structural levels was small and in most cases less than the scatter in the test measurements. Since the method of removing modal excitation in the test was to rapidly move the rotating mass speed away from the mode frequency, rather than instantly switch off the excitation, repeatability of damping estimates from the Moving Block was inferior to that in the rotor-on tests. Frequency results were similarly flat, but with a trend of fall-off in torsion frequency at high speed, giving a mean reduction in measured frequency of 0.24 Hz at 68.6 m/s, compared with 0 m/s. There is evidence that inclusion of this effect may improve the final level of agreement between test and theory (see Section 5.1, below).

4.4 Single Blade Mode Set

In the CSA stability predictions for the Model 3 tests, The measured trim conditions at each *test point have been applied in calculating sets of blade modes. For each test point the correct* collective pitch and resulting steady loads, and hence structural couplings, are then reproduced in the J134 blade modes program. Typically, the applied collective pitch varied from around zero at zero wind to 46° at the highest test speed. The resulting effects of such a large change in orientation of sections was significant, on both frequencies and shapes of the fundamental flap and lag modes of the cantilevered blade. This is illustrated in Table 4, for the zero and highest speed test points for the 900 rpm zero delta-3 case.

Table 4 Effect of Forward Speed on Blade Modes - Predictions from Program J134

Rotating Cantilevered Single Blade

Run no.	Airspeed (m/s)	Frequency (Hz)	Frequency (/rev)	Tip Deflections Flap	Tip Deflections Lag
23.03	0.0	25.9	1.73	1.00	-0.157
		28.2	1.88	0.254	1.00
24.11	68.7	22.4	1.50	-0.491	1.00
		30.9	2.06	1.00	0.325

In earlier stability predictions for the model, and for the full-scale EUROFAR aircraft, a single set of blade modes, for the trim conditions of the highest speed point, had been used for the full speed range. This was considered a valid approximation, since the main concern was to predict the stability boundary at high speed. In Figures 13 (frequencies) and 14 (damping), stability predictions using a single blade mode set in this way are compared with the datum multiple-set predictions, and with test. The differences seen for points below the highest speed are relatively small, confined mainly to the wing torsion frequency and the chord and torsion frequency behaviour at high speed. It can be seen that the damping results provide a valid representation. From these results, the use of multiple-set predictions would only be necessary when some insight into modal interactions or damping below the stability boundary is required.

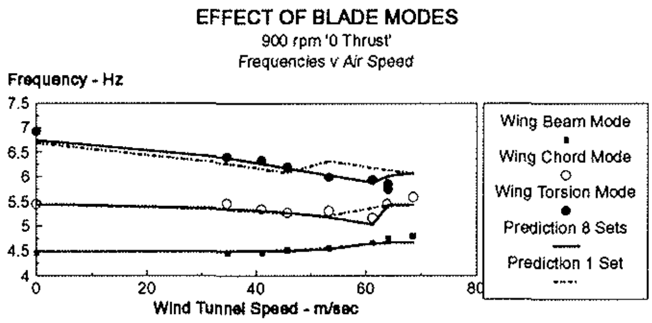

Figure 13

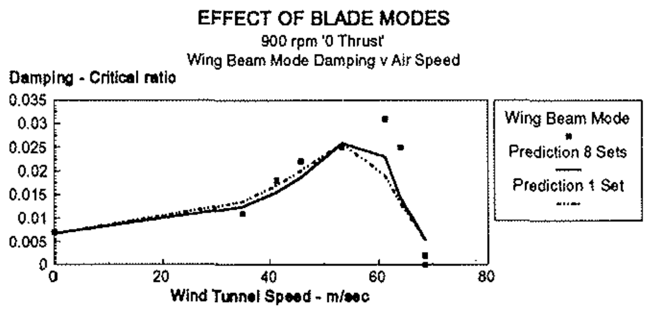

Figure 14

4.5 Gimbal Stiffness

The stiffness of the rotor hub gimbal for Model 3 is made up of the combined effects of the elastomeric gimbal bearing and the bellows drive. From a static test, this stiffness was measured as 2655 lbf.in/rad (300 Nm/rad), while matching a predicted blade mode to the in-situ rap test gave a dynamic value of 3144 lbf.in/rad. For the stability predictions a datum value of 3000 lbf.in/rad was assumed. This equates to a fundamental cyclic flap mode frequency in hover of 1.06 per rev.. As a sensitivity assessment, predictions were also made for a stiffness of 2000 lbf.in/rad (frequency 1.04 per rev.). Results for stiffnesses of 3000 and 2000 are shown in Figures 15 (frequencies) and 16 (damping). Included in these plots are values for the highly damped regressing lead-lag/gimbal mode. This mode is predominantly a cyclic lead-lag mode at low airspeed, acquiring a significant amount of gimbal motion as air speed is increased.

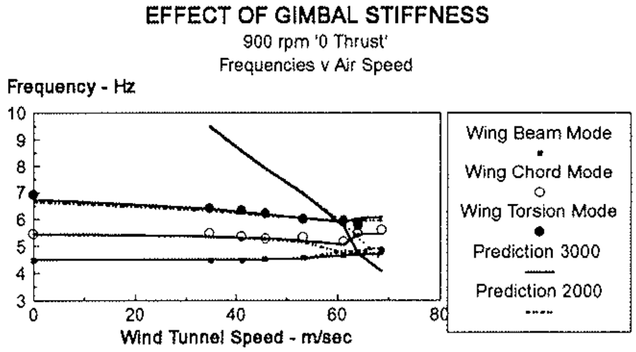

Figure 15

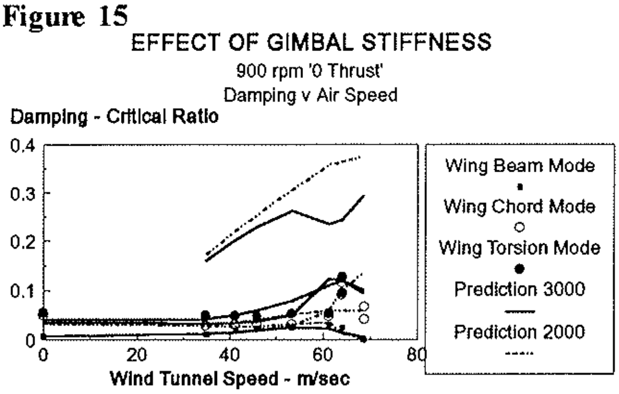

Figure 16

Although the regressing mode was too highly damped to be detected during the wind tunnel test, during which only the more lightly damped progressing lead-lag mode could be found, it is clear from the datum prediction that the frequency behaviour of the wing modes (in particular the wing chord mode) indicates the cross-over locations with the regressing mode. It should be noted that the frequencies have been presented in a cross-over form rather than a coalescence form, on the basis that the lightly-damped modes are always designated as the wing modes. In practice the predicted regressing mode shape shows a high degree of coupling with degrees of freedom in the wing modes. The wing modes, from measurement and prediction, show correspondingly high levels of gimbal and lead-lag motion at high speeds. Comparison with the predictions for a stiffness of 2000 shows that the reduced gimbal stiffness has a significant effect on the wing mode frequencies at high speed in the cross-over region, with associated strong effects on wing torsion mode damping as well as the damping of the regressing mode, but little effect on wing beam mode damping. The higher gimbal stiffness gives better agreement with test, for both frequencies and damping values of the wing modes.

5 COMPARISONS OF TEST AND THEORY

Comparisons of test and theory are presented for stability of Model 3, using the CSA predictions with the UN-standard structural model, and for blade loads in the conversion regime, using predictions from R150 with synthesis from harmonics.

5.1 Stability

Results for the five tested configurations (Table 1) are presented in Figures 17-26. Predictions for the 'zero-thrust' cases include use of multiple blade mode sets, defined at the trim conditions of each test point, while those for the '67 N' cases use a single mode set, defined at the trim condition for the test point at the highest speed.

For the 900 rpm 'zero-thrust' case (Figures 17-18), frequency agreement between prediction and test is good, with only the highest speed torsion frequency prediction being slightly high. The regressing lead-lag rotor mode is shown on the frequency plot as a single measured point at zero wind and the full speed range for the prediction. Agreement at the single point is good. Values at non-zero wind speeds were not measured due to the high damping in this mode (above 15% critical), but the influence of the crossing point is seen in the other measured frequencies above 60 m/s, particularly in the wing chord mode. Damping agreement between prediction and test is good for the wing beam mode, with a small over-prediction of the speed for instability. For the other wing modes, the trend of increased damping at high speeds is captured by the prediction, including the damping reduction in the chord mode at the highest speed (where there is no torsion test point for comparison). Detailed agreement is less good in these modes, although it should be noted that at the higher levels of damping (above 4%), accuracy of damping measurement is reduced. Although structural damping levels based on the flutter check (without the rotor) were used for predictions, agreement in chord and torsion is poor at zero speed in this case. This may be due to behaviour of the splined driveshaft, damping the chordwise motion, with more effect at zero speed due to a lower level of vibratory torque. The results for the case based on the nominal 67 N cruise thrust (Figures 19-20) are similar to those at 'zero-thrust', with a good overall level of agreement between measurements and predictions. The regressing mode is omitted from the plots, since the blade mode set used in the predictions is only correct at high speed. Deviations in frequency agreement at low to mid speeds should also be assessed in this light. There is a trend of

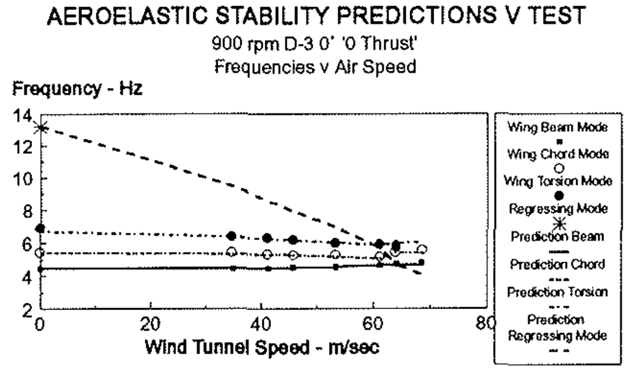

Figure 17

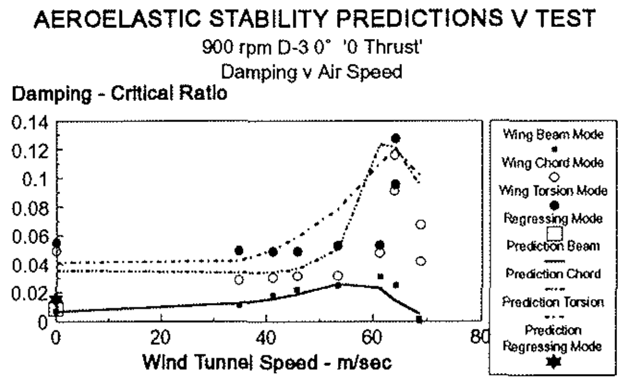

Figure 18

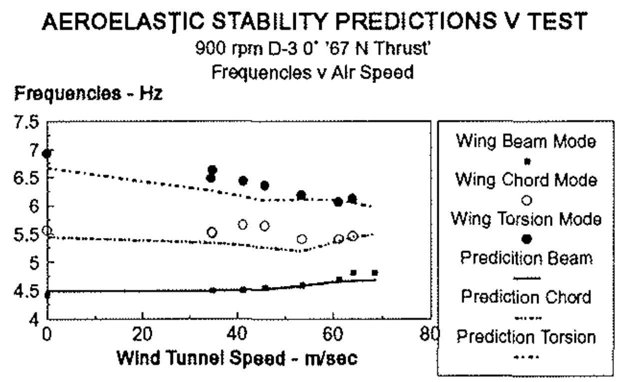

Figure 19

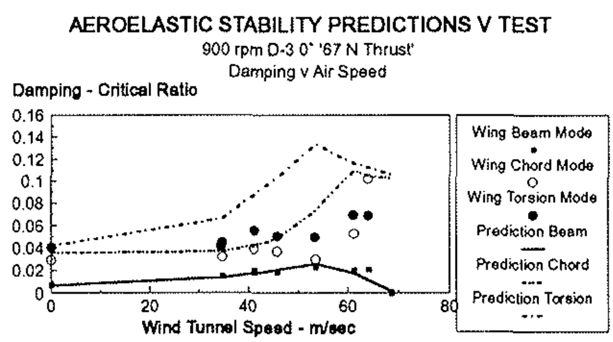

Figure 20

over-prediction of damping in the wing torsion mode at high speed, although measured levels are again high enough to degrade accuracy of the Moving Block estimates.

For the 1124 rpm 'zero-thrust' case (Figures 21-22), frequency agreement between test and prediction is good, except for over-prediction of wing torsion frequencies at high speed, above the regressing mode cross-over, suggesting that couplings in the theoretical torsion mode may

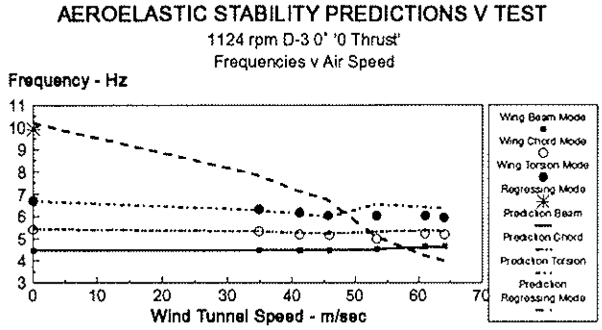

Figure 21

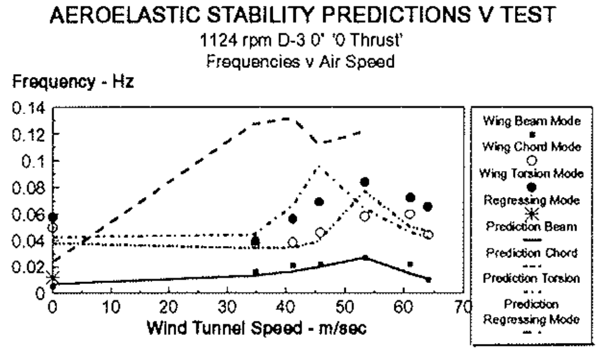

Figure 22

be inaccurate. Damping agreement is also good, with only detail of the torsion mode at high speed and the chord and torsion values at zero wind showing discrepancies. The predicted regressing mode damping is more fully described in this plot, since much of the values are below 15%. Measurements of the lead-lag mode in the test were however confined to those for the more lightly damped progressing mode, which is outside the plotted frequency range. A single point at zero wind has been attributed to the regressing mode.

For the changed delta-3, from zero to 20°, the results at 900 rpm and 'zero thrust' (Figures 23-24) show the significant reduction in the speed for instability. The delta-3 effectively

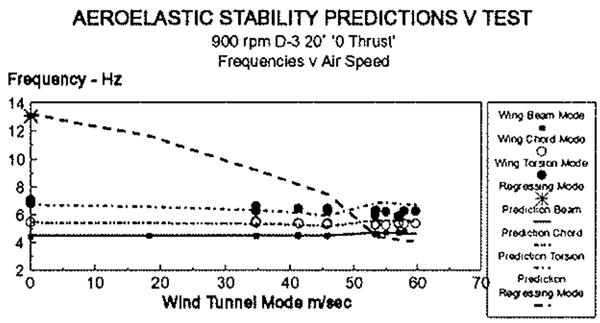

Figure 23

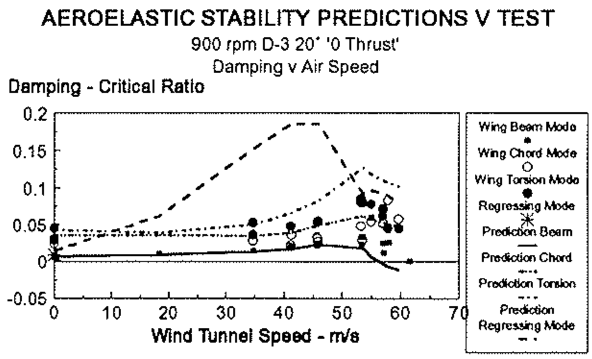

Figure 24

introduces an aerodynamic stiffness term to the gimbal tilting, changing the manner in which the destabilising aerodynamic forces act on the rotor with increased airspeed. The destabilising effect of the coupling is over-predicted by the analysis, such that the predicted instability speed is approximately 5 m/s (8%) low. The predictions also tend to over-estimate wing torsion mode frequencies and damping at high speeds. It is difficult to be conclusive about the measured maximum beam damping, since it is dependent on speed resolution in the data. Taking these discrepancies into account, the overall agreement between measurements and predictions is still good. For the same configuration at a nominal 67 N of thrust (Figures 25-26), similar comments apply. The use of a single blade mode set for this case degrades

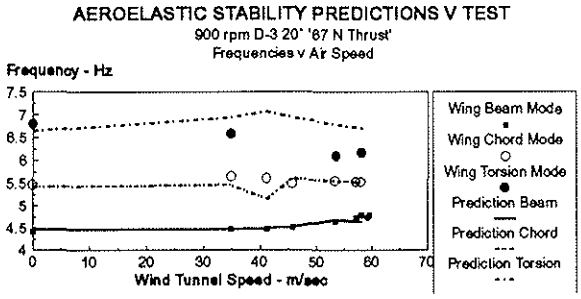

Figure 25

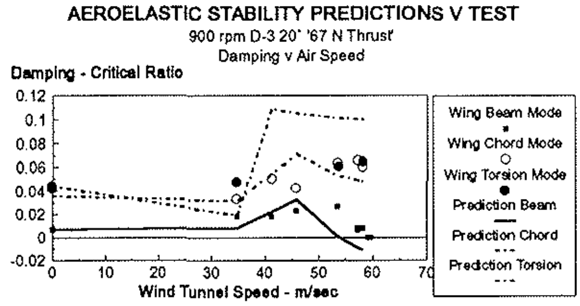

Figure 26

frequency agreement at the mid speed range, particularly placing the regressing mode cross-over at too low a speed, affecting chord and torsion results. However, as seen in Section 4.4, above, this method does not degrade prediction accuracy in the important high-speed area. There appears to be a clearer degradation of beam mode stability with increased thrust for this configuration, from both test and theory, than for the zero delta-3 cases.

In summary, good overall agreement between measured and predicted values of frequencies and damping has been achieved over the full case set. Given that the theoretical structural model, without the rotor, was optimised for only one of the five cases, this provides a good level of validation for the theoretical methods, and in particular for the CSA program. There is a pattern over the whole case-set to over-predict wing torsion frequency and damping at high speed, to over-predict the beam mode instability speed for zero delta-3 slightly, and to under-predict it for 20° of delta-3.

5.2 Blade Loads

Loads data were recorded in the tests for 16 conditions in the conversion flight regime. The 3 highest speed high-thrust conditions were identified as high speed boundary points (Reference 1). Results for 2 of these points, at 30° and 60° nacelle tilts, are presented here as examples. For each point, the gimbal tilt was trimmed to zero, rotor speed was 1124 rpm and delta-3 was 20°. Measured loads and corresponding predictions are included as follows:

Run no.	Nacelle tilt (deg)	Airspeed (m/s)	Figure Numbers Moments Flatwise	Edgewise	Torsion
25.62	30	44.3	27	28	29
26.24	60	43.3	30	31	32

For run 25.62, moments are plotted against blade radius as mean and half peak-to-peak values.

For run 26.24, averaged moment waveforms are plotted against azimuth, for a single blade station.

From the plots of radial distributions (Figures 27-29), it can be seen that agreement between test and prediction is quite good for flatwise moments. Half peak-to-peak edgewise moments agreement is almost equally as good, while steady mean edgewise predictions show significant disagreement with test. Reasons for this disagreement have yet to be determined. Conversely, for the steady torsion moments agreement is good, while half peak-to-peak values are grossly under-predicted. This latter result is to be expected, since the data for the

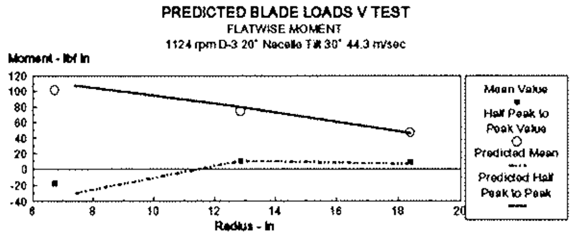

Figure 27

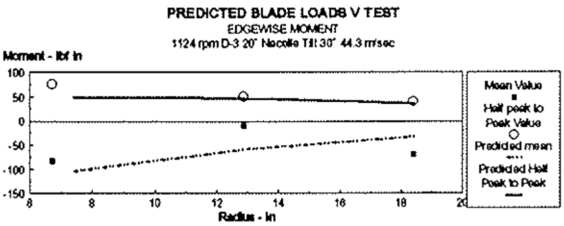

Figure 28

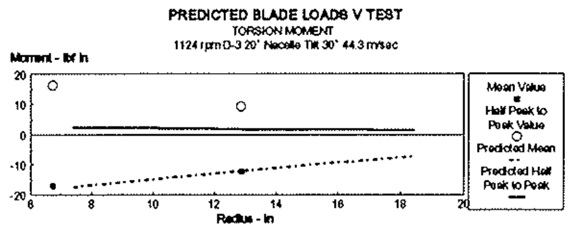

Figure 29

(uncambered) NACA0012 aerofoil used as an approximation cannot reproduce the pitching moment characteristics of the actual (cambered) NACA 64-series aerofoils. It would be instructive to repeat the calculations with aerofoil data more representative in this respect.

The waveform results (Figures 30-32) again show that levels of vibratory flatwise and edgewise moments are predicted well. There is evidence of a difference between predicted and measured mean levels of flatwise moment, and of a phase difference, particularly in the edgewise moment. This is of significant interest, since the approximate treatment of the gimbal in the prediction does not include the theoretical Coriolis loading alleviation of a homokinetic drive. These results, also seen for

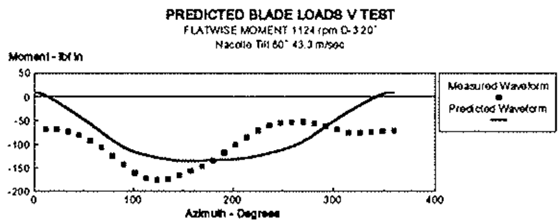

Figure 30

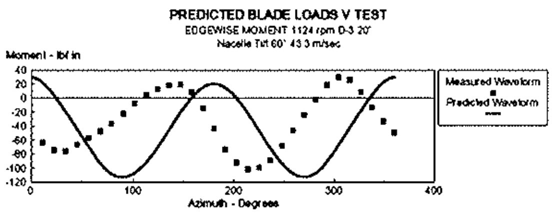

Figure 31

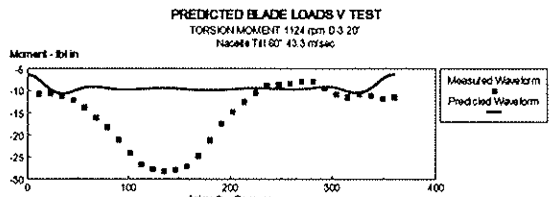

Figure 32

other conversion conditions, suggest that this alleviation is small in magnitude but seen more clearly in phase. As expected, the torsion moment waveform reflects the aerofoil approximation, with the prediction failing to capture a once-per-rev pitching moment event centred around 130° of azimuth, but otherwise giving a fair representation of the underlying level.

Given that these loads prediction results represent an approximate application of a helicopter rotor code with minimal modifications, the overall levels of agreement, particularly in the vibratory flatwise and edgewise moments, are encouraging.

6 CONCLUSIONS

Further analysis of the Model 3 test data at WHL by the Moving Block method, using output from blade strain gauges, has reduced scatter in torsion mode damping results and confirmed chord mode trends in the previous test-site analysis, completing the processing of the test point set.

The test results show wing beam mode instability at high airspeed, with trends of increased damping in chord and torsion modes and evidence of regressing rotor mode crossover also in the high speed range. The speed for instability is significantly reduced by a change from zero delta-3 to 20° delta-3, but relatively insensitive to changes in thrust and rotor speed.

WHL stability and blade loads prediction methods have been successfully applied to the test conditions. Stability predictions are very sensitive to details of the dynamic model of the non-rotating structure, and in particular to wing torsion frequency and beam/torsion couplings, with a lesser dependence on beam/chord and chord/torsion couplings.

Stability predictions are also sensitive to blade aerodynamic tip relief assumptions and hub gimbal dynamic stiffness. Ultimate stability margins can be successfully predicted using a single blade mode set defined at the highest airspeed, although multiple sets are required to represent the full speed range. For Model 3, there is evidence that inclusion of wing aerodynamics in the prediction would improve torsion mode representation at high speed.

Application of a helicopter rotor loads prediction code to the conversion regime, with minimal modifications and use of a harmonic synthesis approximation, has yielded encouraging results, particularly with respect to agreement of vibratory edgewise and flatwise moments with test. Evidence from these results suggests that Coriolis alleviation from the homokinetic gimbal drive is only significant in the phase of the resultant loading.

Overall agreement with test has provided a good level of validation of the CSA stability prediction method, and also identified areas for improvement. The exercise has highlighted the need for sensitivity studies when modelling a full-scale aircraft at the design stage, particularly of the structural dynamics aspects, and for early and accurate correlation of wing/fuselage structural dynamics models with test.

7 ACKNOWLEDGEMENTS

The author would like to express his gratitude to colleagues at Westland Helicopters for their contributions to this work, and in particular to Steve Holton, for his invaluable role as author of the analysis and code of CSA. EUROFAR is part-funded by the UK Department of Trade and Industry and is a EUREKA project of the European Union.

8 REFERENCES

1) Jessop D A C, et al., Wind Tunnel Testing of a EUROFAR Tilt Rotor Aeroelastic Stability Model.
Paper presented at 19th European Rotorcraft Forum, 1993
2) Juggins P T W, et al., Experimental Activities to Support the EUROFAR Tilt Rotor Project Preliminary Phase.
Paper presented at the Royal Aeronautical Society EUROFAR 1 Day Conference, 1989.
3) Holton S A, et al., An Anglo-French Rotor Blade Stability Workshop, Using Different Prediction Methods and Test Results.
Paper presented at 50th AHS Annual Forum, 1994.
4) Hansford R E, Rotor Load Correlation with the British Experimental Rotor Program Blade. AHS Journal, 1987.
5) Lau B H, et al., Correlation of the Lynx XZ170 Flight-Test Results up to and beyond the Stall Boundary.
Paper presented at 49th AHS Annual Forum, 1993
6) Juggins P T W, Substantiation of the Analytical Prediction of Ground and Air Resonance Stability of a Bearingless Rotor, using Model Scale Tests.
Vertica Vol. 14, 1990
7) Bousman W G, et al., Application of the Moving Block Analysis.
USAAVRADCOM 81-0653
8) Acree C W, et al., Identification of XV-15 Aeroelastic Modes using Frequency-Domain Methods.
Paper presented at 14th European Rotorcraft Forum, 1988